Biogeosciences, 13, 4219–4235, 2016
www.biogeosciences.net/13/4219/2016/
doi:10.5194/bg-13-4219-2016

Biogeosciences Open Access EGU

Long-term drainage reduces CO_2 uptake and increases CO_2 emission on a Siberian floodplain due to shifts in vegetation community and soil thermal characteristics

Min Jung Kwon[1], Martin Heimann[1,2], Olaf Kolle[1], Kristina A. Luus[1,3], Edward A. G. Schuur[4], Nikita Zimov[5], Sergey A. Zimov[5], and Mathias Göckede[1]

[1]Biogeochemical Systems, Max Planck Institute for Biogeochemistry, Jena, Germany
[2]Division of Atmospheric Sciences, Department of Physics, Helsinki University, Helsinki, Finland
[3]Centre for Applied Data Analytics Research (CeADAR), Dublin Institute of Technology, Dublin, Ireland
[4]Center for Ecosystem Science and Society, and Department of Biological Sciences, Northern Arizona University, Flagstaff, AZ, USA
[5]North-East Science Station, Pacific Institute for Geography, Far-Eastern Branch of Russian Academy of Science, Chersky, Republic of Sakha (Yakutia), Russia

Correspondence to: Min Jung Kwon (mkwon@bgc-jena.mpg.de)

Received: 7 December 2015 – Published in Biogeosciences Discuss.: 18 January 2016
Revised: 17 June 2016 – Accepted: 30 June 2016 – Published: 26 July 2016

Abstract. With increasing air temperatures and changing precipitation patterns forecast for the Arctic over the coming decades, the thawing of ice-rich permafrost is expected to increasingly alter hydrological conditions by creating mosaics of wetter and drier areas. The objective of this study is to investigate how 10 years of lowered water table depths of wet floodplain ecosystems would affect CO_2 fluxes measured using a closed chamber system, focusing on the role of long-term changes in soil thermal characteristics and vegetation community structure. Drainage diminishes the heat capacity and thermal conductivity of organic soil, leading to warmer soil temperatures in shallow layers during the daytime and colder soil temperatures in deeper layers, resulting in a reduction in thaw depths. These soil temperature changes can intensify growing-season heterotrophic respiration by up to 95 %. With decreased autotrophic respiration due to reduced gross primary production under these dry conditions, the differences in ecosystem respiration rates in the present study were 25 %. We also found that a decade-long drainage installation significantly increased shrub abundance, while decreasing *Eriophorum angustifolium* abundance resulted in *Carex* sp. dominance. These two changes had opposing influences on gross primary production during the growing season: while the increased abundance of shrubs slightly increased gross primary production, the replacement of *E. angustifolium* by *Carex* sp. significantly decreased it. With the effects of ecosystem respiration and gross primary production combined, net CO_2 uptake rates varied between the two years, which can be attributed to *Carex*-dominated plots' sensitivity to climate. However, underlying processes showed consistent patterns: 10 years of drainage increased soil temperatures in shallow layers and replaced *E. angustifolium* by *Carex* sp., which increased CO_2 emission and reduced CO_2 uptake rates. During the non-growing season, drainage resulted in 4 times more CO_2 emissions, with high sporadic fluxes; these fluxes were induced by soil temperatures, *E. angustifolium* abundance, and air pressure.

1 Introduction

Arctic ecosystems have long acted as carbon sinks due to their consistent low air temperatures (T_a) and the presence of permafrost that both inhibit the mineralization of soil carbon. Although Arctic net primary production and standing biomass are smaller than those of adjacent climate zones (Saugier et al., 2001), the low decomposition rates of Arctic ecosystems have resulted in an accumulation over 1000 Pg

of belowground organic carbon in the upper 3 m of the soil in permafrost regions (Hugelius et al., 2014; Schuur et al., 2015). However, the tendency for Arctic ecosystems to take up more CO_2 on average than they release may be changing due to global climate change, which has given rise to shifts in T_a and precipitation patterns. While the photosynthetic rates and standing biomass in the Arctic have become larger (Epstein et al., 2012; Jia, 2003; Myneni et al., 1997; Xu et al., 2013), the rate of organic carbon decomposition has also increased (Bond-Lamberty and Thomson, 2010), which could potentially accelerate CO_2 cycle processes. Further, it is not only a matter of how fast CO_2 circulates between the atmosphere and the upper soil layers but also what will happen to the massive amount of stored carbon (Schuur et al., 2009). Thus, understanding how CO_2 flux patterns of Arctic ecosystems change as a consequence of climate change, as well as how this affects the fate of permafrost carbon, is of great importance (Abbott et al., 2016; Koven et al., 2011; Schuur et al., 2008, 2015).

Gross primary production (GPP) is chiefly determined by the length of the growing season (Baptist and Choler, 2008; White et al., 1999; Xia et al., 2015) and leaf area index (LAI; Barr et al., 2004); secondary influences are water and nutrient availability, as well as local climate conditions such as T_a and radiation (Chapin et al., 2012a). As each plant species responds differently to changes in the aforementioned factors controlling GPP, and as successional changes in vegetation species distribution may take place under a changing climate, the total amount of carbon assimilated (net primary production, NPP), and plant respiration (autotrophic respiration, R_a) may undergo changes. The rate of organic matter decomposition (heterotrophic respiration, R_h) increases under warmer and more aerobic conditions, and is also influenced by the quality of available organic matter. If any of these conditions are modified due to climate change, the rate of R_h may also change in response.

Warming T_a have been observed in the Arctic (Serreze et al., 2000), and disproportionately warmer conditions are forecast in response to climate change (Collins et al., 2013; Kirtman et al., 2013; Overland et al., 2014). As noted in the preceding paragraph, rates of both photosynthesis and organic matter decomposition have increased with warmer T_a (Belshe et al., 2013; Bond-Lamberty and Thomson, 2010; Epstein et al., 2012; Jia, 2003; Myneni et al., 1997; Xu et al., 2013), and these trends are predicted to continue. This has the potential to change Arctic terrestrial ecosystems from a carbon sink to a source, with accelerated organic carbon decomposition as a dominant process (Koven et al., 2011; Schaefer et al., 2011). Schuur et al. (2015) predict that, under the current climate warming trajectory, $\sim$ 5–15 % of the permafrost carbon pool may be released into the atmosphere by 2100.

An increase in T_a can have an immediate impact on soil hydrology, potentially adding complexity to the drivers of CO_2 fluxes and the permafrost carbon pool. In permafrost regions, land surface warming is usually followed by topographical changes, and thus the formation of small-scale local hydrological conditions; wetter microsites can form due to subsiding ground following permafrost thaw (Jorgenson et al., 2006; O'Donnell et al., 2011), while adjacent areas become drier as water drains laterally to subsided areas. These phenomena are particularly pronounced when increased T_a thaws ice-rich permafrost, such as ice wedges and ice lenses (Liljedahl et al., 2016). In some Arctic regions, changing precipitation patterns can aggravate or offset this situation. Precipitation in the Arctic has been generally increasing over the last 5 decades (Kattsov and Walsh, 2000), but patterns are fluctuating across both time and space (Curtis et al., 1998; Stafford et al., 2000); at times, the surface water balance has also been found to be decreasing (Oechel et al., 2000). Although, overall, greater precipitation is expected in the Arctic as the result of intensified hydrological cycles under climate change, the net effect may significantly vary by region (Bintanja and Selten, 2014; Huntington, 2006; Kirtman et al., 2013). Different areas in the Arctic may therefore become either wetter or drier through the combined effects of atmospheric warming and permafrost thaw, as well as varying rates of precipitation.

Several studies have investigated the effects of drainage on CO_2 fluxes in the Arctic (Table 1). Field water table depth (WTD) manipulation experiments and comparison studies with varying WTD have generally shown decreased net CO_2 uptake or increased net CO_2 emission at lower water levels, primarily due to increased ecosystem respiration (R_{eco}; Christensen et al., 2000; Huemmrich et al., 2010; Kim, 2015; McEwing et al., 2015; Oechel et al., 1998; Olivas et al., 2010; Zona et al., 2011); in most cases, GPP increased as well. Although some studies have shown slightly increased net CO_2 uptake when the increase in GPP is larger than the increase in R_{eco} under drier conditions (Natali et al., 2015), the magnitude of the increase in R_{eco} is usually larger than that of GPP (Christensen et al., 2000; Huemmrich et al., 2010; Kim, 2015; McEwing et al., 2015; Oechel et al., 1998; Olivas et al., 2010; Zona et al., 2011). The between-site variability of changes in net ecosystem exchange (NEE) presented in Table 1 can be attributed to differences in the observation period, vegetation type, as well as the intensity and duration of WTD changes in the specific studies. Microcosm experiments have also shown inconsistent results, with a decrease in water level resulting in either decreased (Johnson et al., 1996) or increased (Peterson et al., 1984) net CO_2 fluxes. These findings exemplify how the net effect of changes in WTD arise from interactions between multiple factors, and can vary strongly depending on vegetation and soil types (Billings et al., 1982). Therefore, although previous studies have shown that WTD reduction affects GPP and R_{eco} rates, the direction and significance of changes in net CO_2 cycling have been found to differ from ecosystem to ecosystem.

Most of the existing field observation and incubation studies (Table 1) have focused on the short-term effects of changes in WTD, with a few exceptions that included per-

Table 1. CO_2 flux changes (g C-CO_2 m^{-2} day^{-1}) in response to a WTD decrease, expressed as either $flux_{control}$–$flux_{lower\text{-}WTD}$ or $flux_{higher\text{-}WTD}$–$flux_{lower\text{-}WTD}$. Negative net CO_2 flux rates represent a net increase in terrestrial CO_2 uptake; positive changes denote a decrease in net CO_2 uptake by the terrestrial ecosystem or an increase in terrestrial CO_2 emissions to the atmosphere. The ranges of these changes are from different years, soil types, and study sites. Numbers in parentheses represent percent change compared to the original (control, WTD condition) flux.

Sites	WTD change	Net CO_2 flux change	Reference
Coastal plain	Drawdown	+0.59 (+160 %)	Huemmrich et al. (2010)
	3 cm lower	+0.23 (+87 %)	Olivas et al. (2010)[2]
	Up to 3.6 cm lower[1]	+1.17 (+63 %)	Christensen et al. (2000)[3]
	7–7.5cm lower	+0.36 to +0.4 (+450 to +500 %)	Oechel et al. (1998)
	8.5 cm lower	+2.99 (+365 %)	Kim (2015)[4]
	11.9 cm lower[1]	+0.41 (+67 %)	Zona et al. (2011)[4]
	20 cm lower[1]	+0.72 (+37 %)	McEwing et al. (2015)
Floodplain	20–35 cm lower	−0.06 (−47 %)	Merbold et al. (2009)[5]
Moist tundra	2.5 cm lower	−0.02 (−3 %)	Natali et al. (2015)[6]
Laboratory	Saturated vs. field capacity	−2.63 to −1.41 (−1716 to −344 %)	Johnson et al. (1996)
	5 cm lower	−0.61 to +0.96 (−59 to +72 %)	Billings et al. (1982)
	10 cm lower	+2.21 (+184 %)	Peterson et al. (1984)

[1] WTD difference from natural variation instead of manipulation. [2] Only data from 2008 were used, as this was the only time when the WTD of the drained area was lower than that of the control area. [3] Only from grassland data. [4] Only R_{eco} was considered (no GPP). [5] Only data from 2003 and 2005 were used, as these were the only years when climate conditions were similar. [6] Only data from 2013 were used, as this was the only time when the WTD of the drained area was lower than that of the control area.

mafrost thaw history (Johnston et al., 2014; Schuur et al., 2009). A further limitation is that most of these studies have been carried out in North America, despite the fact that permafrost regions in Eurasia not only cover about twice the area but also contain twice the amount of carbon as compared to North America (Tarnocai et al., 2009). Drying manipulation experiments in the Eurasian Arctic with timescales of decades or more will therefore greatly contribute to understanding drainage effects on CO_2 fluxes in Arctic ecosystems. In addition to these growing-season CO_2 fluxes, several studies have highlighted significant contributions of non-growing-season CO_2 emissions to the annual CO_2 budget in the Arctic (Coyne and Kelley, 1971; Kelley et al., 1968; Panikov and Dedysh, 2000; Webb et al., 2016; Zimov et al., 1993, 1996). Because of the insulation provided by snow, soil temperatures (T_{soil}) remain warmer compared to T_a, and biological processes may continue throughout the non-growing season (Kelley et al., 1968; Webb et al., 2016; Zimov et al., 1993, 1996). Non-growing-season fluxes are also affected by state changes from water to ice (Mastepanov et al., 2013). However, no studies have yet compared non-growing-season CO_2 fluxes between wet and dry sites.

As a continuation of hydrological manipulation initiated a decade ago in northeastern Siberia (Merbold et al., 2009), the present study investigates how 10 years of drainage have affected ecosystem structure and CO_2 fluxes. By directly comparing CO_2 fluxes of a pristine area to those from the drained area, our results go beyond a mere description of the immediate disturbance effects, and clearly point out differences between the properties of pristine and drained ecosystems. These differences highlight how the disturbed area has adapted to persistently drier conditions. Our investigation is focused on shifts in T_{soil}, thaw depths (TDs), and vegetation community structure, as well as how these changes then influence net CO_2 exchange and its component fluxes, GPP and R_{eco} (Fig. 1). In addition to the growing season, phenomena during the non-growing season will be also described; this represents the first drying manipulation experiment of this nature that extends beyond the growing season.

2 Methodology

2.1 Site description

The study site is located in a Kolyma River floodplain near Chersky, northeastern Siberia (also written as Cherskii or Cherskiy). The dominant vegetation species are tussock-forming *Carex appendiculata* and *lugens*, and *Eriophorum angustifolium*. An organic peat layer (15–20 cm deep) has accumulated on top of alluvial material soils (composed of silty clay), although some organic peat materials can be found within alluvial layers due to cryoturbation.

Based on the record filtered by the Berkeley Earth project (berkeleyearth.org, station ID 169921) for the period 1960–2013, mean monthly T_a at the Chersky weather station ranged between −33 °C in January and +13 °C in July, and the annual mean T_a was −11 °C. World Meteorological Organization (WMO) records for the period 1950–1999 indi-

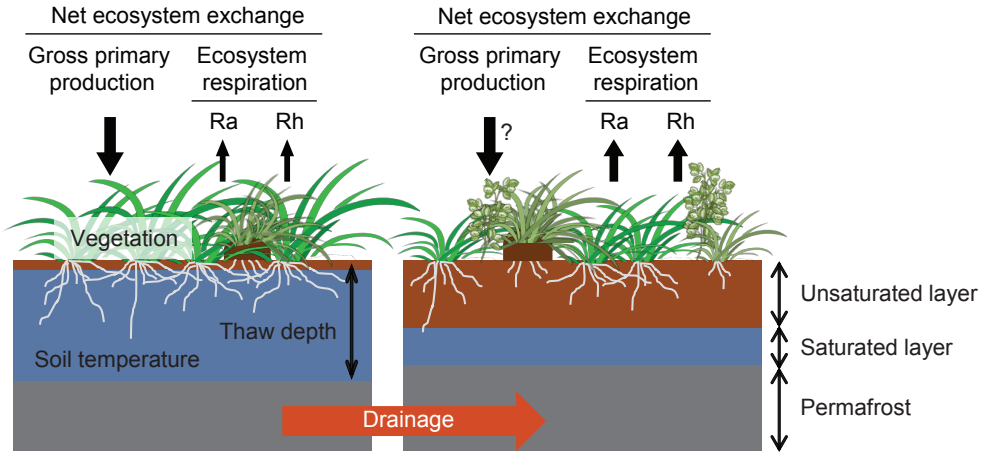

Figure 1. A schematic showing how a decade-long drainage installation affects a floodplain ecosystem and CO_2 fluxes. Drainage of a floodplain ecosystem alters T_{soil} through changing heat capacity and thermal conductivity, with increased T_{soil} in shallow layers, decreased T_{soil} in deeper layers, and shallower TDs, as well as decreasing the abundance of wetland grasses while increasing the abundance of shrubs. These modifications will subsequently affect CO_2 fluxes by changing the rates of GPP and possibly increasing R_{eco}, which consists of R_a and R_h.

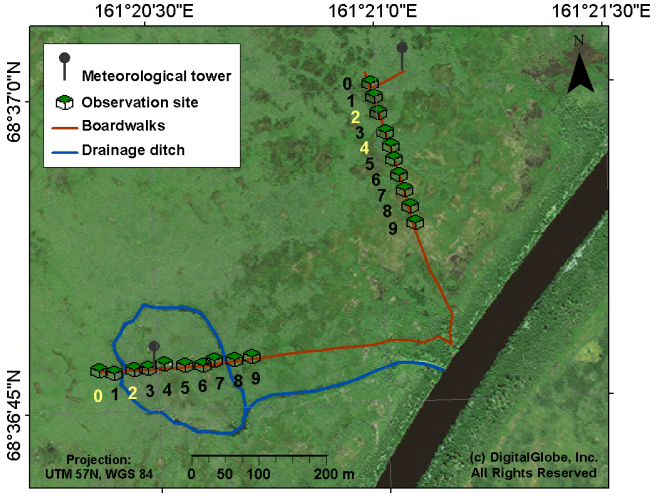

Figure 2. Aerial photograph of the site, including schematics of the drained (bottom left) and the control (top right) transects. Names of plots are written with numbers and two core plots for more frequent flux measurements are highlighted in yellow in each transect. Fluxes, vegetation community structures (created using a non-destructive method), WTDs, and TDs were measured in all plots, and T_{soil} were measured in even-numbered plots only.

cate a total annual precipitation of 197 mm, with about half of this falling as rain in summer. Snowmelt at the site and in the surrounding river basin usually results in a spring flood. This flooding brings an increased water level of up to 50 cm above the soil surface in late May or early June, followed by a gradual decrease in the water level starting in early July. After the flood waters have receded, the primary water source is precipitation.

A drainage ring with a ~200 m diameter and minimum depth of 50 cm was constructed in fall 2004 (Merbold et al., 2009), to drain water into the nearest river channel (Ambolikha). As a result, WTD in this drained area is lowered by 20 cm on average and by up to 30 cm in the growing season compared to control areas (Merbold et al., 2009). While the spatial range of drainage effects varies by soil topography, high-resolution land cover classification (WorldView with 2 m resolution; Richards and Xiuping, 1999) has indicated a high abundance of vegetation groups dominant in dry areas to only within 200 m on both sides of the ditch (Burjack et al., unpublished data); we can therefore limit the drainage effect to this maximum distance. Starting summer 2013, we measured ecosystem properties and CO_2 fluxes at two sites in parallel (Fig. 2): the drained area affected by the ditch since 2004 (68°36′47″ N, 161°20′29″ E), and a control area (68°37′00″ N, 161°20′59″ E) approximately 600 m away from the drained area that is not affected by the drainage ditch. Despite some short-term diurnal fluctuations of up to a few centimeters following evapotranspiration, as well as precipitation events and water supply from thawing permafrost, distinct differences in WTD between these treatment areas persist over the growing season. Each transect of 10 plots in the drained and control areas (henceforth referred to as drained and control transects, respectively) was selected using a stratified systematic sampling method. First, we selected 10 approximate positions with 25 m intervals along the boardwalks or transects; we then selected the final plots by considering representative vegetation groups of the selected positions, and by selecting specimens small enough to fit within flux chambers (Table 2 and Fig. 2). All plots were located within ca. 2 m of boardwalks to minimize disturbances.

Table 2. WTD and vegetation characteristics of plots. Vegetation groups were created by taking into account only *Carex* sp., *E. angustifolium*, and shrubs when the relative abundance of each species exceeded 10 %. The relative abundances of consisting plant species (mean ±SD) are separately presented. Average WTD was calculated by pooling all WTD measurements from both years (mean ±SD), except the period where the whole area was flooded from snowmelt. When the average WTD of the growing season was larger than −10 cm, plots were classified as wet groups.

Transect	Plot ID no.	Vegetation group	Vegetation abundance (%)	Average WTD (cm)	WTD group	Group abbr.
Drained	0	EriophorumShrub	90, 10	4.6 ± 2.2	Wet	Drained_wet
	1, 2, 4	CarexEriophorum	31 ± 23, 64 ± 21	-14.1 ± 8.4	Dry	Drained_dry
	3, 5, 6, 7, 8, 9	Carex	82 ± 30	-19.2 ± 6.1	Dry	Drained_dry
Control	0	CarexShrub	85, 15	-1.3 ± 2.3	Wet	Control_wet
	1, 3, 6, 7, 8, 9	Eriophorum	79 ± 33	4.3 ± 2.4	Wet	Control_wet
	2	EriophorumShrub	80, 20	3.9 ± 2.1	Wet	Conrol_wet
	4, 5	CarexShrub	71 ± 12, 27 ± 15	-18.5 ± 4.1	Dry	Control_dry

We conducted three field campaigns. The first was 3 weeks, starting on 20 July 2013 (representing the mid-growing season); the second was 4 weeks, starting on 1 November 2013 (representing the non-growing fall season); and the third was 10 weeks, starting on 15 June 2014 (representing the growing season). The non-growing season was defined as the time period when the average daily T_a was below 0 °C. Although WTD of the drained transect was generally lower by 20 cm than that of the control transect after the spring flood in both years, heterogeneous soil topography rendered varying WTD within each transect: one plot in the drained transect had an average WTD close to that of wet plots in the control transect, and two plots in the control transect had an average WTD close to that of dry plots in the drained transect. Since our objective was to analyze how a decade-long drainage disturbance affects CO_2 fluxes and its links to environmental parameters, we categorized 20 plots into four groups – drained(D)_wet, drained_dry, control(C)_wet, and control_dry – according to transect and WTD category (Table 2). Plots were classified as "dry" when the average WTD of the growing season was lower than −10 cm. In 2013, all 20 plots were observed with equal frequency to investigate spatial variability among plots; in 2014, four core plots (i.e., one plot from each group; Table 2) were more frequently observed to highlight temporal variability over the growing season (Table 2 and Fig. 2). Due to different lengths of the observation periods between the two years, we divided data from 2014 into three subseasons to distinguish seasonal variability: (2014.1) 15 June–5 July, (2014.2) 6 July–26 July, and (2014.3) 27 July–20 August. Subseason 2014.3 and the 2013 field campaign covered similar periods, based on an analysis of plant phenology with the normalized difference vegetation index (NDVI), and both periods included peak growing season (i.e., when the NDVI of the site was the highest).

2.2 CO_2 flux measurements

At each plot, a $60 \times 60\,cm^2$ polyvinyl chloride (PVC) collar was inserted 15 cm into the ground in late June 2013, 3 weeks before the first flux measurements. No noticeable plant damage was identified around the collars after installation, and 3 weeks was expected to provide enough buffer time for any stabilization needed in the event of minor belowground damage (Högberg et al., 2001; Parkin and Venterea, 2010). To take the flux measurements, a transparent chamber (60 cm on each side, made of 4 mm thick plexiglass) was placed on the collar. The chamber had an opening valve on the top to avoid pressure effects when we placed the chamber onto the collars. Sensors for T_a, air humidity, air pressure (P_a), and photosynthetically active radiation (PAR) were attached to one side of the chamber and all parameters were measured in parallel with fluxes. These sensors – along with three small fans on a vertical pole attached in one of the corners, for the purpose of mixing the air inside – were placed such that their shadows would not bias incoming solar radiation. CO_2 flux was measured with a non-steady-state flow-through (i.e., closed dynamic) method using an Ultra-Portable Greenhouse Gas Analyzer (UGGA, Los Gatos Research, USA), and all data were recorded at 1 Hz with a CR1000 data logger (Campbell, USA).

We restricted each flux measurement to a maximum of 2 min to minimize saturation effects (i.e., warming and pressurized effects) within the chamber. In the event of strong incoming radiation, which can cause T_a to increase more than 1 °C per minute, we placed ice packs on the collar rims inside the chamber to keep T_a constant while measuring fluxes. The number of ice packs was adjusted by observing the T_a changes at 1 Hz frequency. In addition to measuring NEE using the transparent chamber, in summer we also measured R_{eco} by covering the chamber with a tarp that blocked incoming radiation. In the non-growing season we did not find significant differences between NEE and R_{eco}, probably due to the role of low temperatures, low solar radiation,

and snow cover in limiting photosynthesis; we therefore measured NEE only with the transparent chamber.

To calculate the CO_2 flux from the observed changes in CO_2 concentrations ($[CO_2]$) within the sampling time of 2 min, median values of the $[CO_2]$ slopes were computed by selecting multiple time windows based on a bootstrapping approach, and fluxes (mg C-CO_2 m^{-2} s^{-1}) were calculated by taking into account T_a, P_a, and the volume and area of the chamber (Rochette and Hutchinson, 2005). Flux rates that fell outside of the range of seasonal mean $\pm 3\sigma$ (i.e., standard deviation) were removed as outliers. GPP and R_{eco} are expressed in positive values, indicating the amount of CO_2 assimilated and respired, respectively. Negative values for NEE denote net CO_2 uptake by the terrestrial ecosystem, while positive values denote net CO_2 emission to the atmosphere.

2.3 WTD, TD, and T_{soil}

WTD was measured during each flux measurement using perforated PVC pipes with a 25 mm diameter, which were installed at each plot. WTD was measured relative to soil surface, with values larger than 0 cm denoting water standing above the soil surface. TD was estimated by pushing a measuring pole into the ground. At every second plot T_{soil} probes were installed at 5, 15, 25, and 35 cm (Th3-s, UMS, Germany), and data were recorded while fluxes were measured.

To investigate the effect of T_{soil} on R_h, we measured respiration rates of soils at 0–15 and 15–30 cm depths by aerobically incubating soils at 15 °C in the laboratory ($N = 6$ for each depth). Respiration rates were corrected for bulk density and average growing-season T_{soil} at each 0–15 and 15–30 cm depth of both the wet and dry plots by assuming a Q_{10} value of 2 as the mean for tundra ecosystems (Zhou et al., 2009). The relative R_h rates between the wet and the dry plots were subsequently compared, and were linked to changes in T_{soil}.

2.4 Vegetation community structure

Changes in vegetation community structure between 2003 (before the drainage ditch was installed) and 2013 (9 years after the drainage ditch was installed) were examined using historical data collected in 2003 through the Terrestrial Carbon Observation System Siberia project (TCOS Siberia; Corradi et al., 2005). Vegetation community structure was then identified in 2013 along the same transect as in 2003 (which had not been drained in 2003, but was drained in 2013), as well as in the control transect (newly selected in 2013). Identification was carried out using the same harvest method in all transects. All living vegetation inside a $1 \times 1\,m^2$ quadrat ($N = 4$ per transect) was harvested. Collected vegetation was sorted by species, completely dried at 40 °C, and then weighed (g dry biomass m^{-2}). Relative abundance of each species (%) was calculated based on the dry biomass to avoid potential biases linked to the water content of plants.

To correlate abundances of plant species with CO_2 fluxes without destroying plots for further flux observations, we applied a non-destructive point-intercept method using a $60 \times 60\,cm^2$ quadrat that was divided into $10 \times 10\,cm^2$ subgrids in 2014. After creating this grid, we recorded the plant species that a laser pointer hit when pointed downward at each subgrid intersection, and calculated the percentage of each species' cover. This analysis was performed within each collar, so that vegetation community structure of each plot could be linked directly to CO_2 fluxes. As plots were selected using a stratified method (see Sect. 2.1), this analysis was also performed at a spot 10 m away from each plot, to confirm that the vegetation community structure of each plot accurately represented the transects.

2.5 Data analysis and interpolation

2.5.1 Interpolation of growing-season CO_2 fluxes

To compare flux variability among plots induced by temporal discrepancies in sampling, and to visualize the implications of these differences for net growing-season CO_2 uptake, CO_2 fluxes for each vegetation and WTD group were interpolated throughout the growing-season observation period. To simulate CO_2 flux rates we adapted a satellite-data-driven CO_2 flux model, the Polar Vegetation Photosynthesis and Respiration Model (PolarVPRM), which calculates high-latitude NEE by subtracting GPP from R_{eco} (Luus and Lin, 2015):

$$\mathrm{GPP} = (\lambda \times T_{scale} \times W_{scale}) \times \mathrm{FAPAR_{PAV}} \times \left(\frac{1}{1+\frac{\mathrm{PAR}}{\mathrm{PAR_0}}}\right) \times \mathrm{PAR} \quad (1)$$

$$\mathrm{T_{scale}} = \frac{(T_a - T_{min}) \times (T_a - T_{max})}{(T_a - T_{min}) \times (T_a - T_{max}) - (T_a - T_{opt})^2} \quad (2)$$

$$W_{scale} = \frac{a \times \mathrm{WTD}}{\mathrm{WTD_{max}} - \mathrm{WTD_{min}}} + b\,(0 < a < 1, a + b = 1), \quad (3)$$

where λ is a parameter representing maximum light use efficiency at low light levels, and $\mathrm{PAR_0}$ represents the half-saturation value of PAR. T_{scale} and W_{scale} are scaling variables ranging between 0 and 1 that reflect the influence of T_a and water availability, respectively, on photosynthesis. The set of three parameters required for calculating T_{scale}, i.e., T_{min}, T_{max}, and T_{opt} were set to 0, 40, and 20 °C according to literature recommendations to avoid the parameter instability that would arise from empirically fitting these parameters, due to the strong positive correlations between T_a and PAR (Mahadevan et al., 2008). $\mathrm{FAPAR_{PAV}}$ is the fraction of PAR absorbed by the vegetation, and is calculated using the Moderate Resolution Imaging Spectroradiometer (MODIS) Enhanced Vegetation Index (EVI).

Site-level meteorological observations of T_a and PAR were used as inputs for PolarVPRM; these observations were taken from sensors installed in the chamber system (for calibration) and from nearby meteorological towers (for temporal interpolation; Fig. 2). The influence of water availability on photosynthesis (W_{scale}) was calculated based on WTD determined next to each plot at the time of flux measurement, with an optimized scaling factor (a, b) to obtain the best fits between $GPP_{modeled}$ and $GPP_{observed}$.

Both parameters (λ and PAR_0) were fitted empirically in R (R Core Team, 2013). PAR_0 was obtained from the curve fit between GPP and PAR measured with flux observations using the nonlinear least squares curve fitting in R (R Core Team, 2013); λ was calculated as the slope of the linear regression of observed GPP, and of GPP calculated from Eq. (1). GPP was estimated excluding PAR terms for CarexEriophorum in 2013 because no positive relationship between GPP and PAR was found (see Sect. 3.3.2). GPP was then computed half-hourly using linearly interpolated WTD and EVI, as well as half-hourly measured T_a and PAR from the meteorological station.

R_{eco} was calculated using an empirical Q_{10} model:

$$R_{eco} = \alpha \times e^{k \times T_a}. \quad (4)$$

The two free parameters in this exponential relationship between R_{eco} and T_a, α and k, were empirically calculated from chamber-based measurements of R_{eco} and T_a using nonlinear least squares curve fitting in R (R Core Team, 2013). Once these coefficients were calculated, R_{eco} was calculated at half-hourly intervals with half-hourly-averaged T_a from the meteorological station at each transect.

Parameter optimization and flux interpolation were carried out separately across four core plots for the year 2014, while 10 plots from each transect were categorized into three vegetation groups and pooled for the year 2013. These vegetation categories took into account only *Carex* sp., *E. angustifolium*, and shrubs when the relative abundance of each species exceeded 10 % (Table 2). The categorized vegetation groups of the drained transect were EriophorumShrub, CarexEriophorum, and Carex, while those of the control transect were CarexShrub, Eriophorum, and EriophorumShrub (Table 2). The period of interpolation was restricted to the observation periods within each year because WTD (W_{scale}) was not measured continuously outside of this period. The discrepancies between the observed and modeled fluxes were calculated using root mean squared error (RMSE) and mean bias error (MBE). All data points that were used for calibration were utilized for the error estimates due to the limited number of data points.

Uncertainty ranges of the interpolated fluxes were calculated using cross validation by creating 2000 data subsets consisting of randomly selected data points (bootstrapping, 80 % of the total data set). To obtain an error range of R_{eco}, the 2000 resulting pairs of parameters, and, subsequently, $R_{eco} \pm 2\sigma$ were computed for each 1 °C T_a bin. Similarly,

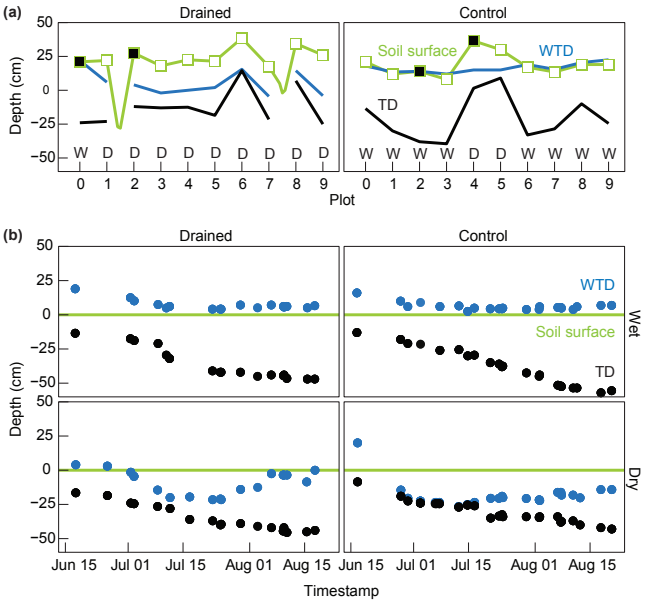

Figure 3. (a) Spatial variability in WTDs and TDs measured across the two transects on 10 August 2013. Plots are indicated with squares (core plots indicate closed squares). The letters W and D indicate the wet and dry WTD category of each plot, respectively. **(b)** Temporal variability in WTD and TD observed at the four core plots over the growing season of 2014, separated by transect (columns) and WTD category (rows).

2000 pairs of PAR_0 and λ were estimated for binned PAR. The range of GPP was subsequently estimated by including the rest of the terms from Eq. (1). To constrain the uncertainty ranges of the interpolated fluxes, we took the GPP and R_{eco} error ranges at each point from the corresponding PAR and T_a bin, respectively, that reflected the current condition. Because NEE is calculated as the difference of GPP and R_{eco}, uncertainty ranges were also determined by adding the two error ranges of GPP and R_{eco}. For CarexEriophorum and EriophorumShrub groups in 2013 – for which no positive relationship between GPP and PAR was found or the number of data points was not enough to produce uncertainty ranges, respectively – the bootstrapping step was skipped.

2.5.2 Statistical analysis

Spatial differences in the 2013 WTD and TD between the two transects were tested using an independent t test. A permutational multivariate analysis of variance (PERMANOVA) was performed to compare vegetation community structure between the drained and the control transects of 2013 and 2003. Data from 2014 were not compared with those from 2003 due to the different experimental methods employed. A two-way analysis of covariance (ANCOVA) was carried out with WTD category (wet and dry) and depth as independent variables, to compare T_{soil} between WTD categories. Correlations between WTD and TD were tested by

taking values from August of each year when TD was the deepest and the effects of WTD were strongest.

To see if vegetation groups affected the 2013 fluxes, all fluxes were aggregated by vegetation group (see Sect. 2.5.1; Table 2) and a one-way analysis of variance (ANOVA) was performed for each vegetation group as an independent variable. When independent variables significantly influenced dependent variables, Tukey's post hoc test was applied. To investigate whether vegetation group and T_{soil} significantly affected the non-growing-season CO_2 fluxes, one-way ANOVA and multiple linear regressions were performed, respectively. A multiple linear regression analysis was also performed to identify additional major environmental drivers for cold-season CO_2 fluxes. For multiple linear regression analyses, significant variables were defined based on the Bayesian information criterion (BIC); with these selected variables the best-fit regression models were identified, based on the Akaike information criterion (AIC). All statistical analyses were performed using R (R Core Team, 2013).

Table 3. ANCOVA results with WTD category (wet and dry), and soil depth (cm) as the independent variables and T_{soil} (°C) as the dependent variable. The time periods of the entire year 2013, as well as three subseasons of 2014 – (2014.1) 15 June–5 July, (2014.2) 6–26 July, and (2014.3) 27 July–20 August – were separately analyzed. The significance of F values are denoted with asterisks (*** $P < 0.001$, ** $P < 0.01$, * $P < 0.05$).

	Transect	WTD	Depth	WTD × Depth
2013	Drained	12.75***	602.64***	13.38***
	Control	15.38***	700.93***	2.64
2014.1	Drained	3.54	169.46***	0.02
	Control	32.55***	165.35***	29.56***
2014.2	Drained	26.21***	400.48***	0.52
	Control	1.24	380.91***	2.42
2014.3	Drained	101.87***	680.50***	7.55**
	Control	6.49*	813.62***	4.91 *

3 Results and discussion

3.1 WTD changes from drainage

Following flooding due to snowmelt in early June, the drainage ditch effectively lowered WTD in the drained transect. Average differences in WTD between the two transects were significant with a mean drop of approximately 20 cm, and a maximum difference of up to 30 cm during a 3-week period in summer 2013 (independent t test, $P < 0.001$, $t = -4.55$, $df = 17.91$; Fig. 3a). Approximately the same difference in mean WTD was observed in the middle of the 2014 growing season. However, several significant rainfall events from late July of 2014 triggered an increase in WTD in the dry plots, especially in the drained transect (Fig. 3b). The amount of precipitation was similar at both transects, but WTD for some drained_dry plots was more susceptible to increases in WTD compared to control_dry plots; this was because the width of the area within the drainage ring was 3 times larger than that of the elevated areas of control_dry plots. In addition, drainage may slow when the water level rises within the drainage ditch due to the obstruction of water flow by taller vegetation – *E. angustifolium* and aquatic plants – at the end of the growing season (Allan, 1995; Green, 2005). As a result, WTD in drained_dry plots stayed high longer than in the control transect following heavy rainfalls. Similar patterns were also observed in 2005, 1 year after the drainage ditch was installed (Merbold et al., 2009). Nonetheless, WTD difference between the wet and the dry plots showed distinct patterns. In the long term, it can be speculated that new drainage pathways will be established, which will lead water away more effectively after precipitation events, and thus reduce the fluctuations in WTD we observed at our site. Transferring our findings to a natural disturbance (e.g., the formation of a connected system of troughs following ice-rich permafrost thaw), we expect that water drainage will be more effective than our drainage manipulation, as thawing permafrost following persistently warmer conditions will induce more pronounced topographical changes (Jorgenson et al., 2006; Liljedahl et al., 2016; O'Donnell et al., 2011).

3.2 Shifts in T_{soil} and TD and their effects on CO_2 fluxes

3.2.1 T_{soil} and TD

Our two-way ANCOVA indicated that drainage resulted in both stronger diurnal fluctuations in T_{soil} in shallow layers and colder T_{soil} in deep layers, as compared to the wet plots (Table 3 and Fig. 4). This finding highlights the important role of water content in the thermal properties of organic soils, with the soil of shallow layers of the dry plots tending to heat up more easily during the daytime due to the reduced heat capacity of dry organic soil (Abu-Hamdeh, 2003; Idso et al., 1975; Lakshmi et al., 2003; Reginato et al., 1976). At the same time, these dry organic soils also have lower thermal conductivity, limiting downward heat transfer; as a result, deeper layers remained colder than soil at the same depth in the wet plots (Abu-Hamdeh, 2003). This mechanism reduced TD in the dry plots, the effect of which became more distinct at the end of the growing season due to the continued effects of WTD (Fig. 5). The positive correlations between WTD and TD in August clearly show this trend (for 2013: $r = 0.47$, $P < 0.05$; for 2014: $r = 0.67$, $P < 0.001$; Fig. 5).

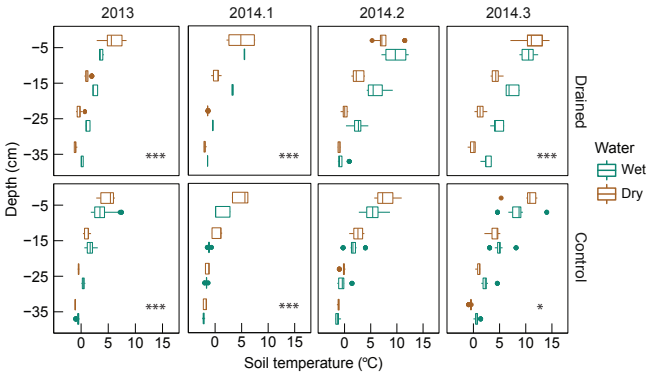

Figure 4. T_{soil} profiles based on observations at 5, 15, 25, and 35 cm depths from even-numbered plots each in the drained (top) and the control (bottom) transects. Boxplot contains median, 25 and 75 % quartiles, and ±1.5 interquartile ranges. To minimize the impact of the diurnal temperature cycle on this temporally discontinuous data set, the time window for averaging was restricted to 13:00–17:00 LT. Panels from left to right show data from 2013, as well as from three subseasons of the growing season of 2014: (2014.1) 15 June–5 July, (2014.2) 6–26 July, and (2014.3) 27 July–20 August. Data subsets where significant differences in WTD between the wet and the dry plots were detected are marked with asterisks (*** $P<0.001$, ** $P<0.01$, * $P<0.05$).

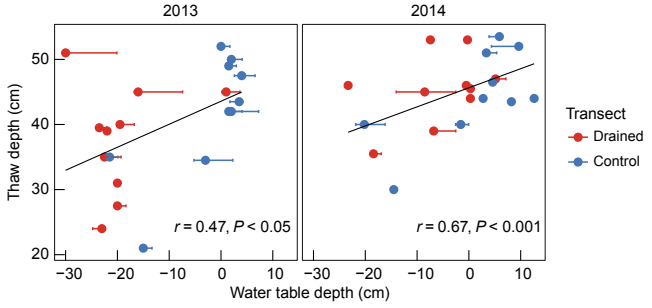

Figure 5. Correlations of TDs and WTDs in mid-August 2013 and 2014. Error bars of WTD represent the minimum and the maximum ranges of WTD of the previous 20 days. Results of correlation analysis for each year are presented with black lines.

3.2.2 T_{soil} and TD effects on CO_2 fluxes

GPP and R_{eco} rates increased with T_{soil} at 5 cm (Fig. 6) because warmer T_{soil} generally accelerates both photosynthesis (Lawrence and Oechel, 1983; Schwarz et al., 1997) and root respiration (Boone et al., 1998). The average R_{eco} rates of the dry plots were 25 % higher than those of the wet plots in 2013 (independent t test, $P<0.001$, $t=-5.70$, $df=532$) despite the fact that GPP rates were found to be lower in the dry plots, meaning that lower R_a rates would have been expected (Fig. 6). This increase in the R_{eco} rates can be partly explained by the increased rates of R_h under more aerobic conditions following drainage: as anaerobic respiration is slower and less efficient than aerobic respiration, carbon release from both organic and mineral soils (surface and deep soil layers, respectively) under aerobic conditions can be 4–10 times higher than under anaerobic conditions (Lee et al., 2012). However, drier conditions altered T_{soil} regimes, and these effects further affected R_h rates.

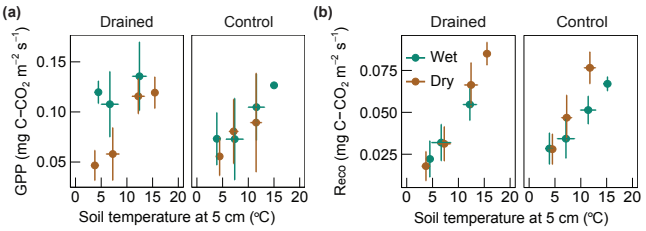

Figure 6. Links between average T_{soil} at 5 cm and **(a)** GPP and **(b)** R_{eco} rates by transect (column). Data are from 2013 (20 July–10 August) and subseason 2014.3 (27 July–20 August); both cover similar phenological periods. Data were grouped into temperature bins of 5 °C.

Modifications in T_{soil} in shallow layers had greater impacts on R_h than those in T_{soil} in deep layers: the warmer T_{soil} in shallow layers of the dry plots increased R_h by 240 %, while colder T_{soil} in deep layers reduced R_h only marginally as compared to the wet plots. Combining these two contrasting effects, R_h rates in dry plots were elevated by 95 % as a result of the stronger effects of T_{soil} in shallow layers as compared to T_{soil} in deep layers on compacted peat soils. This increase was largely due to a greater amount of organic carbon – an increased total carbon content by 11 % as well as more compacted soil with an increase in bulk density by 44 % (data not shown) – in the dry plots affected by warmer T_{soil} in shallow layers. Contrary to the accelerated respiration rates at the surface, colder T_{soil} in deep layers and reduced TDs imply that carbon currently stored in permafrost can be preserved following drainage. In addition to these contrasting effects, another opposing influence of the physical structures of vegetation on T_{soil} – for example, the negative relationship between shrub abundance and TD due to shade (Blok et al., 2010) and the positive relationship between shrub abundance and TD due to decreased albedo (Bonfils et al., 2012) – with continuously changing vegetation communities following drainage (see Sect. 3.3) need to be monitored over a longer period of time to gain further insight into the net impact of secondary drainage on carbon accumulation and CO_2 fluxes.

3.3 Shifts in vegetation community structure and its effects on CO_2 fluxes

3.3.1 Vegetation community structure

In its natural, undisturbed state, the vegetation community of this floodplain has historically been dominated by *Eriophorum angustifolium*, followed by *Carex appendiculata* and *lugens*. This vegetation community structure was reflected in the observations made in 2003 (Corradi et al., 2005) – that

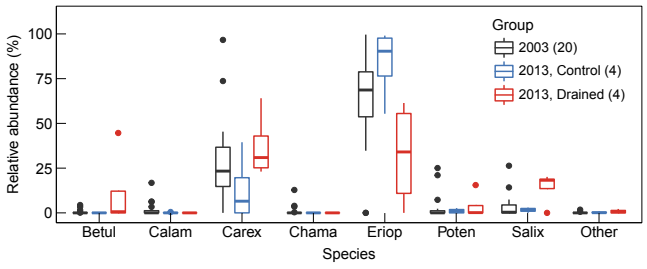

Figure 7. Abundances of vegetation species observed across the transects in 2003 and 2013. Numbers in parentheses are the number of replicates. Boxplot contains median, 25 and 75 % quartiles, and ±1.5 interquartile ranges. Betul: *Betula exilis*, Calam: *Calamagrostis purpurascens*, Carex: *Carex* species, Chama: *Chamaedaphne calyculata*, Eriop: *Eriophorum angustifolium*, Poten: *Potentilla palustris*, Salix: *Salix* species.

is, before the drainage ditch was constructed (Fig. 7, black) – as well as in the control transect in 2013 (Fig. 7, blue). After a decade of drainage, the abundance of *E. angustifolium* decreased, while shrubs (*Betula exilis*, and *Salix fuscescens* and *pulchra*) and *Carex* sp. became the dominant species in the drained transect (Fig. 7, red). While no statistically significant differences were found between the vegetation community structures in 2003 and in the control transect of 2013 (PERMANOVA, $F = 1.62$, $P = 0.19$), significant differences were found between both the 2003 and the drained transect of 2013 (PERMANOVA, $F = 3.31$, $P < 0.05$) and between the two transects of 2013 (PERMANOVA, $F = 5.22$, $P < 0.05$). Although we did not experimentally compare the two observation methods (see Sect. 2.4), a qualitative comparison of results from 2013 (i.e., harvest) and 2014 (i.e., point intercept) showed a similar abundance of each species; this implies that these two different methods can be used to compare vegetation community structures.

In the control transect, the vegetation community structures of the wet and the dry plots were dominated by *E. angustifolium* and *Carex* sp., respectively, but some dry plots within the drained transect showed a vegetation transition stage (Table 2). Plots in the drained transect that were categorized as CarexEriophorum (Table 2) showed a mixture of young *Carex* sp. (without discrete tussock forms or small developing tussocks) and short and thin *E. angustifolium*. The presence of this mixture implies that these areas were formerly dominated by *E. angustifolium*, which is abundant in water-saturated areas, but whose abundance decreased due to drainage. The core plots that were selected based on drainage manipulation and WTD category represented this vegetation shift well; control_wet and drained_wet were dominated by *E. angustifolium*, control_dry was dominated by *Carex* sp. and shrubs, and drained_dry showed a transition stage from *E. angustifolium* to *Carex* sp. (Table 2).

We underestimated the abundance of shrubs (*B. exilis* and *Salix* sp.) within the collars in the drained transect as a result of the methodological choice to exclude tall shrubs when selecting plots to ensure that all of the vegetation could fit into the chambers when measuring fluxes (note that these results are presented to compare CO_2 fluxes by vegetation group; see Sect. 2.4). The abundance of shrubs within the collars of the drained transect was 2 % on average, while independently investigated average abundance along the transect was 20 % on average. This discrepancy will be taken into account in the following sections when interpreting the effects of shrubs on CO_2 fluxes.

3.3.2 Vegetation effects on CO_2 fluxes

Chamber-based CO_2 flux measurements during the 2013 growing season showed similar mean and standard deviations of NEE, GPP, and R_{eco} rates between the two transects (Fig. 8). However, fluxes showed a large variability across plots within each transect (each of which was ca. 225 m), which results from one-way ANOVA indicated to be closely linked to the dominant vegetation groups (NEE: $F = 24.99$, $P < 0.001$; Fig. 8a). R_{eco} also differed by dominant vegetation group, but this difference was not as pronounced as it was for GPP (GPP: $F = 11.23$, $P < 0.001$; R_{eco}: $F = 3.63$, $P < 0.01$; Fig. 8b, c).

One of the vegetation effects on CO_2 fluxes was that, *Eriophorum*-dominated plots in both transects had higher rates of photosynthetic uptake than *Carex*-dominated plots. GPP rates of EriophorumShrub were 55 % higher than those of Carex in the drained transect, and those of EriophorumShrub and Eriophorum were 20 % higher than those of CarexShrub in the control transect in 2013 (Fig. 8b). In 2014, conversely, GPP rates of CarexShrub were 5 % higher than those of EriophorumShrub in the control transect, but this difference was insignificant (Table 4). Thus, the decrease in *E. angustifolium* as a result of drainage generally reduced carbon accumulation in the terrestrial ecosystem. CarexEriophorum plots in the drained transect – which represent a vegetation transition from *E. angustifolium* to *Carex* sp. following drainage – showed the lowest GPP rates in both years, despite the presence of *E. angustifolium* (Fig. 8b). In this transition stage (which is characterized here by declining *E. angustifolium*) or in early succession stages, plants assimilate less CO_2 than they previously did due to lower biomass, and can be more susceptible to disturbances (Chapin et al., 2012b; Niinemets, 2010). The dry and warm year of 2013 was an especially good example of this process: these plots showed slightly decreased GPP rates along with increasing PAR (Fig. S1 in the Supplement), implying that the combination of high PAR and high T_a caused water stress to plants. Under the same climate conditions, CarexShrub in the control transect – which can be considered to be the potential vegetation communities of CarexEriophorum groups – took up significantly less CO_2 than in 2014, but did not show decreasing GPP rates (Fig. S1). This implies that when *E. angustifolium* is fully replaced by *Carex* sp. and shrubs, the cur-

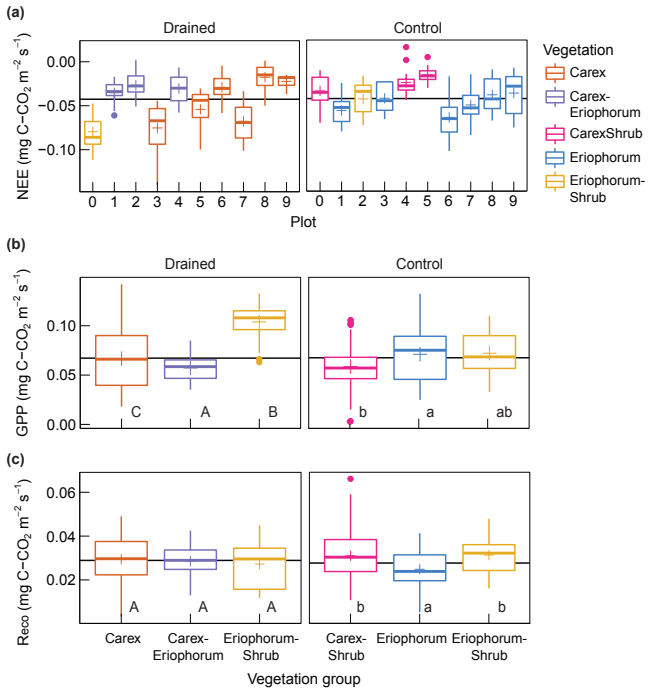

Figure 8. **(a)** Variability of NEE among individual plots during the 2013 growing season. Boxplot contains median, 25 and 75 % quartiles, ±1.5 interquartile ranges, as well as mean values with cross points per plot. The black horizontal bars show the mean flux rates averaged for the entire transect. **(b)** GPP and **(c)** R_{eco} rates aggregated by the vegetation group. Significance of differences between groups, determined by one-way ANOVA and Tukey's post hoc test, is indicated by the letters. Different letters indicate significant differences between groups while the same letters indicate significant similarities.

rent CarexEriophorum plots may not undergo water stress as easily as they currently do although they can be still strongly influenced by climate. Taking into account such transition effects after 10 years of drainage is important given that the fraction of these areas of the total area – 3 out of 10 plots – is not small. Moreover, this finding highlights the fact that ecosystem adaptation to new environmental conditions may take a long time, as 10 years was evidently not sufficient for this ecosystem to be resistant to disturbances, e.g., harsh climate conditions.

Increasing shrub abundance slightly compensated for lowered GPP rates in drained areas following a reduction in *E. angustifolium* coverage. EriophorumShrub of the control transect, which had 10 % shrub coverage, had, on average, 4 % higher GPP rates than Eriophorum in 2013, although this difference was not significant (Fig. 8b). This difference is expected to be larger if the abundance of shrubs was not underestimated (see Sect. 3.3.1). Also, this compensation may become larger with increasing abundance and biomass of shrubs following continuing drainage. Increasing the abundance of shrubs not only changes carbon exchange rates between the atmosphere and the terrestrial ecosystem but also carbon storage patterns within the terrestrial ecosystem (Shaver and Jonasson, 2001). In the drained transect, living aboveground biomass – the sum of leaf and stem – was larger than in the control transect, and in 2003, while the biomass of green leaves decreased, that of stems increased, mostly due to the increased abundance of shrub species (Fig. S2). When shrubs continue to expand, a large portion of carbon will be stored in plants, especially in shrubs' stems, and the proportion of litter added to the soil will decrease accordingly (Fig. S2). The subsequent effects of these changes, such as litter quantity and quality added to soils and its decomposability (Hobbie, 2008; Schädel et al., 2014), need to be further investigated to better understand long-term vegetation effects on CO_2 fluxes.

3.4 Growing-season CO_2 fluxes

3.4.1 Gap-filled growing-season CO_2 fluxes

The modeled fluxes for both 2013 and 2014 had similar patterns to the observed fluxes: *Eriophorum*-dominated plots (i.e., wet plots) generally showed higher GPP rates than *Carex*-dominated plots (i.e., dry plots) in both transects (Table 4). In addition, the 10 % difference in shrub cover between Eriophorum and EriophorumShrub from the control transect did not significantly affect GPP rates (Table 4). R_{eco} rates were consistently greater in the dry plots, in part due to increased R_h rates, and the cumulative R_{eco} increased with drainage by 5 % in 2013 and by 10 % in 2014 (Table 4). Combining the effects of vegetation and T_{soil} on GPP and R_{eco} rates, the net effects of drainage on CO_2 fluxes (NEE) was -0.3 g C-CO_2 m^{-2} day^{-1} (i.e., 25 % more CO_2 uptake) in 2013 and $+0.98$ g C-CO_2 m^{-2} day^{-1} (i.e., 35 % less CO_2 uptake) in 2014 when daily CO_2 fluxes of 20 days, weighted by the number of plots of each group, were compared (Table 4). This range was comparable to other drainage studies presented in Table 1. However, the net CO_2 flux changes were in opposite directions in these two years due to control_dry (CarexShrub) plots' sensitivity to dry and warm conditions during the 2013 observation periods (see Sect. 3.3.2), as well as pooling of the wet and the dry plots to compare changes in flux rates for transect level. Despite the variability between years for transect level, patterns of underlying processes were consistent: after 10 years of drying manipulation, the replacement of *E. angustifolium* by *Carex* sp., more aerobic conditions, and increased T_{soil} in shallow layers all weakened CO_2 uptake and increased CO_2 emission (Table 4).

Table 4. Average daily flux (g C-CO_2 m^{-2} day^{-1}) from interpolation for the period of 22 July–10 August (20 days) in both 2013 and 2014. Values in parentheses are cumulative flux (g C-CO_2 m^{-2}) for the period of 22 July–10 August (20 days) in 2013 and 16 June–20 August (66 days) in 2014. Results represent the fits of all data points ±SD from bootstrapping. NEE was calculated by subtracting GPP from R_{eco}: positive values are net CO_2 emission to the atmosphere, and negative values are net CO_2 uptake by the terrestrial ecosystem.

Year	Group	R_{eco}	GPP	NEE
2013	D_Carex	2.03 ± 0.10 (41 ± 2)	3.42 ± 0.00 (68 ± 0)	-1.38 ± 0.09 (-28 ± 2)
	D_CarexEriophorum	1.89 ± 0.16 (38 ± 3)	3.30 (66)*	-1.41 ± 0.24 (-28 ± 5)*
	D_EriophorumShrub	1.88 ± 0.53 (38 ± 11)	4.81 (96)*	-2.93 ± 0.34 (-59 ± 7)*
	C_CarexShrub	2.04 ± 0.08 (41 ± 2)	2.55 ± 0.02 (51 ± 0)	-0.51 ± 0.05 (-10 ± 1)
	C_Eriophorum	1.76 ± 0.05 (35 ± 1)	3.41 ± 0.01 (68 ± 0)	-1.65 ± 0.04 (-33 ± 1)
	C_EriophorumShrub	2.34 ± 0.17 (47 ± 3)	3.32 ± 0.00 (66 ± 0)	-0.98 ± 0.14 (-20 ± 3)
2014	D_wet (EriophorumShrub)	3.27 ± 0.16 (184 ± 9)	7.59 ± 0.11 (404 ± 6)	-4.31 ± 0.05 (-221 ± 3)
	D_dry (CarexEriophorum)	3.51 ± 0.19 (200 ± 9)	5.14 ± 0.07 (274 ± 4)	-1.64 ± 0.11 (-74 ± 5)
	C_wet (EriophorumShrub)	2.81 ± 0.24 (162 ± 14)	5.85 ± 0.03 (312 ± 1)	-3.05 ± 0.21 (-150 ± 13)
	C_dry (CarexShrub)	3.98 ± 0.21 (222 ± 12)	6.20 ± 0.03 (331 ± 2)	-2.22 ± 0.18 (-109 ± 10)

* As no bootstrapping was conducted on data for GPP, error range in NEE is only from R_{eco}.

3.4.2 Model error from interpolation

Comparing observed against modeled flux rates for all individual measurements in the database, the mean RMSE of R_{eco} was 0.009 and 0.007 mg C-CO_2 m^{-2} s^{-1} for 2013 and 2014, respectively, and that of GPP was 0.021 and 0.016 mg C-CO_2 m^{-2} s^{-1} for 2013 and 2014, respectively (Table S1 in the Supplement). Low uncertainty ranges imply that variations in R_{eco} and GPP can be mainly explained by T_a and PAR, respectively. The uncertainty ranges of R_{eco} were large compared to those of GPP (Table S1), suggesting that R_{eco} rates varied with factors other than T_a, while GPP rates mostly varied with PAR. Larger RMSE and MBE in the drained transect in 2013 compared to the control transect can be attributed to the pooling of data points by vegetation group, as well as to the limited number of data points; the large error in GPP for the Carex group of the drained transect can be attributed to varying standing biomass, and that of the EriophorumShrub in the drained transect stems from the small number of data points (Table S1). In 2014, data points for each group came from only a single plot, but varying WTD and thickening TD over the growing season resulted in relatively large errors (Table S1).

3.5 Non-growing-season CO_2 fluxes

Due to the low T_a and weak solar radiation, GPP in the non-growing season was negligible. Although a limited amount of photosynthetic activity could have theoretically taken place during this time (Atanasiu, 1971), no significant differences were found between NEE and R_{eco}, implying that CO_2 fluxes consisted mostly of CO_2 released from the soil. The drained transect emitted an average of 4 times more CO_2 than the control transect: if the observed flux pattern is representative of the entire month of November, the net CO_2 emission of this month would be 11 g C-CO_2 m^{-2} in the drained transect and 3 g C-CO_2 m^{-2} in the control transect.

Some plots in the drained transect showed sporadically high fluxes, the rates of which were comparable to R_{eco} rates from the growing season (Fig. 9). These high fluxes in the drained transect could be linked to vegetation groups, especially the abundance of *E. angustifolium*, as well as to P_a and T_{soil} (multiple linear regression, adj. $R^2 = 0.46$, $P < 0.001$; P_a, $P < 0.001$; T_{soil} at 5 cm, $P < 0.001$; *Eriophorum*, $P < 0.001$; $P_a \times T_{soil}$ at 5 cm, $P < 0.001$; $P_a \times$ *Eriophorum*, $P < 0.001$). This may be a part of the physical processes outlined by Mastepanov et al. (2008, 2013), through which the freezing of soil pushes stored CO_2 and CH_4 gases in soil to the atmosphere through cracks in soil or dead plant bodies. Although T_{soil} between 0 and 35 cm was consistently below zero, T_{soil} at 35 cm did not fall below −5 °C until the end of November. Ongoing freezing at greater depths than 35 cm and low P_a could have stimulated CO_2 emission from the soil to the atmosphere through dead *E. angustifolium*. The fact that the CO_2 fluxes were influenced by T_{soil} implies that high CO_2 emissions were not exclusively triggered by the physical expression of existing CO_2 in soils, but also from ongoing respiration at relatively mild T_{soil} insulated by snow (Kelley et al., 1968; Webb et al., 2016; Zimov et al., 1993, 1996). CO_2 fluxes in the control transect were also influenced by the abundance of *E. angustifolium*, P_a, and T_{soil} (multiple linear regression, adj. $R^2 = 0.21$, $P < 0.001$; T_{soil} at 5 cm, $P < 0.01$; T_{soil} at 15 cm, $P < 0.01$; T_{soil} at 25 cm, $P < 0.01$; *Eriophorum*, $P < 0.05$; T_{soil} at 5 cm × *Eriophorum*, $P < 0.001$; T_{soil} at 15 cm × *Eriophorum*, $P < 0.001$; T_{soil} at 25 cm × *Eriophorum*, $P < 0.001$), but the rates were relatively constant over time and without high sporadic fluxes, unlike in the drained transect (Fig. 9).

Although the CO_2 fluxes in the non-growing season were partially explained by vegetation group, P_a, and T_{soil}, the

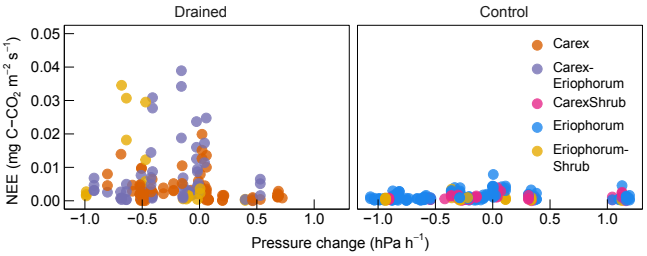

Figure 9. Change in P_a and NEE from November 2013 by vegetation type. Changes in P_a refer to changes within 6 h before individual NEE was measured.

amount of variation (R^2) together explained by these factors was low. We also cannot firmly conclude that the observed sporadic high CO_2 fluxes in November were largely driven by these factors, because we did not observe CO_2 fluxes continuously along with T_{soil}; what is more, these high CO_2 fluxes were only observed in the drained transect despite there being similar conditions in the control transect. High uncertainties and limitations in predicting both non-growing-season CO_2 fluxes and possible high CO_2 fluxes during the thawing season (Friborg et al., 1997) need to be addressed to determine the net effects of drainage on the annual CO_2 fluxes of this site. Nevertheless, the observed considerably higher CO_2 fluxes in the non-growing season for the drained transect imply that drainage not only affects growing-season CO_2 fluxes but also has the potential to alter non-growing-season fluxes significantly.

4 Conclusion and final remarks

Drainage of a floodplain near Chersky resulted in an average WTD drop of 20 cm. This substantially altered both biogeophysical and biogeochemical ecosystem properties over the span of a decade, with profound net impacts on CO_2 fluxes. The first change important for CO_2 processes was that vegetation community structure in the drained areas shifted significantly toward increased *Carex* sp. and shrubs (*B. exilis* and *Salix* sp.) and decreased *E. angustifolium*. The second change was that WTD variation led to divergent T_{soil} profiles by depth, with the drained areas showing greater fluctuations in T_{soil} in shallow layers due to their low heat capacity, and with deeper soil demonstrating colder T_{soil} due to the low thermal conductivity of the dry soil above it. Consequently, the drained areas had shallower TDs compared to the control areas.

These aboveground and belowground changes significantly affected CO_2 fluxes. The drained areas showed higher R_{eco} due to more aerobic conditions, with a greater amount of organic carbon affected by warmer T_{soil} in shallow layers. Dominant plant species in the drained areas took up less CO_2 (i.e., *Carex* sp. engaged in less GPP) than *E. angustifolium*, which is dominant in the control wet areas. Increased abundance of shrubs slightly compensated for the decrease in GPP, but, in our data sets, it could not fully balance out the losses. Overall, drainage increased net CO_2 uptake (NEE) by 25 % in 2013 but decreased it by 35 % in 2014 during the 20 days of the growing season when the two transects were compared. The opposite patterns of the two years can be attributed to control_dry plots, which showed large variations with climate. Despite the inter-annual variability, both years had consistent trends toward the replacement of *E. angustifolium* with *Carex* sp., more aerobic conditions, and increased T_{soil} in shallow layers, all of which weakened CO_2 uptake and increased CO_2 emission. In the non-growing season, CO_2 emission was 4 times larger in the drained than in the control areas, partially as a result of the abundance of *E. angustifolium*, P_a, and T_{soil}.

Ecosystem changes after 10 years of drainage on an Arctic floodplain decreased CO_2 uptake and increased CO_2 emission in both the growing and non-growing seasons. These findings highlight the importance of considering the changes in ecosystem properties under persistent dry conditions when investigating CO_2 fluxes in response to global climate changes. As ongoing global warming thaws ice-rich permafrost and makes some regions drier, Arctic wetlands may accumulate less carbon in the terrestrial ecosystem, respire more CO_2 from shallow soil layers, and preserve carbon in deep soil layers. Given that vegetation communities continue changing after 10 years, with different areas then responding differently to climates, further observations of this site, as well as of other ecosystems in the Arctic, are needed over a longer term to better predict the fate of the Arctic in the face of global climate changes.

5 Data availability

Data are available upon request (mkwon@bgc-jena.mpg.de).

The Supplement related to this article is available online at doi:10.5194/bg-13-4219-2016-supplement.

Acknowledgements. This work has been supported by the European Commission (PAGE21 project, FP7-ENV-2011, grant agreement no. 282700, and PerCCOM project, FP7-PEOPLE-2012-CIG, grant agreement no. PCIG12-GA-2012-333796), the German Ministry of Education and Research (CarboPerm-Project, BMBF grant no. 03G0836G), the International Max Planck Research School for Global Biogeochemical Cycles (IMPRS-gBGC), and the AXA Research Fund (PDOC_2012_W2 campaign, ARF fellowship M. Göckede). The authors wish to express their appreciation to NESS staff members, especially Galina Zimova, Nastya Zimova, and Vladimir Tatayev for organizing and assisting with field work; Chiara Corradi and Lutz Merbold for giving us valuable advice; Martin Hertel, Frank Voigt, Waldemar Ziegler, and other Freiland

group members for technical support; Ina Burjack for providing an aerial map and growing-season partitioning scheme with vegetation phenology, as well as for assisting with field and lab work; Marcus Wildner, Carsten Schaller, and Fanny Kittler for assisting with field work; Mirco Migliavacca for advice on data analysis; Ines Hilke and other RoMA group members for soil analysis; Silvana Schott for assisting with plotting; and Julia McMillan for the language editing. We ordered our authors according to both the first–last author emphasis and equal contribution (i.e., alphabetical sequence) methods (Tscharntke et al., 2007).

The article processing charges for this open-access publication were covered by the Max Planck Society.

Edited by: P. Stoy
Reviewed by: three anonymous referees

References

Abbott, B. W., Jones, J. B., Schuur, E. A. G., Chapin III, F. S., Bowden, W. B., Bret-Harte, M. S., Epstein, H. E., Flannigan, M. D., Harms, T. K., Hollingsworth, T. N., Mack, M. C., McGuire, A. D., Natali, S. M., Rocha, A. V, Tank, S. E., Turetsky, M. R., Vonk, J. E., Wickland, K. P., Aiken, G. R., Alexander, H. D., Amon, R. M. W., Benscoter, B. W., Bergeron, Y., Bishop, K., Blarquez, O., Breen, A. L., Buffam, I., Cai, Y., Carcaillet, C., Carey, S. K., Chen, J. M., Chen, H. Y. H., Christensen, T. R., Cooper, L. W., Cornelissen, J. H. C., de Groot, W. J., DeLuca, T. H., Dorrepaal, E., Fetcher, N., Finlay, J. C., Forbes, B. C., French, N. H. F., Gauthier, S., Girardin, M. P., Goetz, S. J., Goldammer, J. G., Gough, L., Grogan, P., Guo, L., Higuera, P. E., Hinzman, L., Hu, F. S., Hugelius, G., Jafarov, E. E., Jandt, R., Johnstone, J. F., Kasischke, E. S., Kattner, G., Kelly, R., Keuper, F., Kling, G. W., Kortelainen, P., Kouki, J., Kuhry, P., Laudon, H., Laurion, I., Macdonald, R. W., Mann, P. J., Martikainen, P. J., McClelland, J. W., Molau, U., Oberbauer, S. F., Olefeldt, D., Paré, D., Parisien, M.-A., Payette, S., Peng, C., Pokrovsky, O. S., Rastetter, E. B., Raymond, P. A., Raynolds, M. K., Rein, G., Reynolds, J. F., Robards, M., Rogers, B. M., Schädel, C., Schaefer, K., Schmidt, I. K., Shvidenko, A., Sky, J., Spencer, R. G. M., Starr, G., Striegl, R. G., Teisserenc, R., Tranvik, L. J., Virtanen, T., Welker, J. M., and Zimov, S.: Biomass offsets little or none of permafrost carbon release from soils, streams, and wildfire: an expert assessment, Environ. Res. Lett., 11, 034014, doi:10.1088/1748-9326/11/3/034014, 2016.

Abu-Hamdeh, N. H.: Thermal properties of soils as affected by density and water content, Biosyst. Eng., 86, 97–102, 2003.

Allan, J. D.: Channels and flow, in: Stream Ecology: Structure and Function of Running Waters, 1–22, Chapman and Hall, 1995.

Atanasiu, L.: Photosynthesis and respiration of three mosses at winter low temperatures, Bryologist, 74, 23–27, 1971.

Baptist, F. and Choler, P.: A simulation of the importance of length of growing season and canopy functional properties on the seasonal gross primary production of temperate alpine meadows, Ann. Bot., 101, 549–559, 2008.

Barr, A. G., Black, T. A., Hogg, E. H., Kljun, N., Morgenstern, K., and Nesic, Z.: Inter-annual variability in the leaf area index of a boreal aspen-hazelnut forest in relation to net ecosystem production, Agric. For. Meteorol., 126, 237–255, 2004.

Belshe, F., Schuur, E. A. G., and Bolker, B. M.: Tundra ecosystems observed to be CO_2 sources due to differential amplification of the carbon cycle, Ecol. Lett., 16, 1307–1315, 2013.

Billings, W. D., Luken, J. O., Mortensen, D. A. and Peterson, K. M.: Arctic tundra a source or sink for atmospheric carbon dioxide in a changing environmnet?, Oecologia, 53, 7–11, 1982.

Bintanja, R. and Selten, F. M.: Future increases in Arctic precipitation linked to local evaporation and sea-ice retreat, Nature, 509, 479–482, 2014.

Blok, D., Heijmans, M. M. P. D., Schaepman-Strub, G., Kononov, A. V., Maximov, T. C., and Berendse, F.: Shrub expansion may reduce summer permafrost thaw in Siberian tundra, Glob. Change Biol., 16, 1296–1305, 2010.

Bond-Lamberty, B. and Thomson, A.: Temperature-associated increases in the global soil respiration record, Nature, 464, 579–582, 2010.

Bonfils, C. J. W., Phillips, T. J., Lawrence, D. M., Cameron-Smith, P., Riley, W. J., and Subin, Z. M.: On the influence of shrub height and expansion on northern high latitude climate, Environ. Res. Lett., 7, 015503, doi:10.1088/1748-9326/7/1/015503, 2012.

Boone, R. D., Nadelhoffer, K. J., Canary, J. D., and Kaye, J. P.: Roots exert a strong influence on the temperature sensitivity of soil respiration, Nature, 396, 570–572, 1998.

Chapin, F. S., Matson, P. A., and Vitousek, P. M.: Plant carbon budgets, in Principles of terrestrial ecosystem ecology, Springer New York, 157–182, 2012a.

Chapin, F. S., Matson, P. A., and Vitousek, P. M.: Temporal dynamics, in Principles of terrestrial ecosystem ecology, Springer New York, 339–367, 2012b.

Christensen, T. R., Friborg, T., Sommerkorn, M., Kaplan, J., Illeris, L., Soegaard, H., Nordstroem, C., and Jonasson, S.: Trace gas exchange in a high-Arctic valley: 1. Variationsin CO_2 and CH_4 flux between tundra vegetation types, Global Biogeochem. Cy., 14, 701–713, 2000.

Collins, M., Knutti, R., Arblaster, J., Dufresne, J.-L., Fichefet, T., Friedlingstein, P., Gao, X., Gutowski, W. J., Johns, T., Krinner, G., Shongwe, M., Tebaldi, C., Weaver, A. J., and Wehne, M.: Long-term Climate Change: Projections, Commitments and Irreversibility, in Climate Change 2013: The Physical Science Basis. Contribution of Working Group I to the Fifth Assessment Report of the Intergovernmental Panel on Climate Change, Cambridge University Press, Cambridge and New York, 2013.

Corradi, C., Kolle, O., Walter, K., Zimov, S. A., and Schulze, E. D.: Carbon dioxide and methane exchange of a north-east Siberian tussock tundra, Glob. Change Biol., 11, 1910–1925, 2005.

Coyne, P. I. and Kelley, J. J.: Release of carbon dioxide from frozen soil to the Arctic atmosphere, Nature, 234, 407–408, 1971.

Curtis, J., Wendler, G., Stone, R., and Dutton, E.: Precipitation decrease in the western Arctic, with special emphasis on Barrow and Barter Island, Alaska, Int. J. Climatol., 18, 1687–1707, 1998.

Epstein, H. E., Raynolds, M. K., Walker, D. A., Bhatt, U. S., Tucker, C. J., and Pinzon, J. E.: Dynamics of aboveground phytomass of the circumpolar Arctic tundra during the past three decades, Environ. Res. Lett., 7, 015506, doi:10.1088/1748-9326/7/1/015506, 2012.

Friborg, T., Christensen, T. R., and Søgaard, H.: Rapid response of greenhouse gas emission to early spring thaw in a subarc-

tic mire as shown by micrometeorological techniques, Geophys. Res. Lett., 24, 3061–3064, 1997.

Green, J. C.: Modelling flow resistance in vegetated streams: review and development of new theory, Hydrol. Process., 19, 1245–1259, 2005.

Hobbie, S. E.: Temperature and plant species control over litter decomposition in Alaskan tundra, Ecol. Monogr., 66, 503–522, 2008.

Högberg, P., Nordgren, A., Buchmann, N., Taylor, A. F., Ekblad, A., Högberg, M. N., Nyberg, G., Ottosson-Löfvenius, M., and Read, D. J.: Large-scale forest girdling shows that current photosynthesis drives soil respiration, Nature, 411, 789–792, 2001.

Huemmrich, K. F., Kinoshita, G., Gamon, J. A., Houston, S., Kwon, H., and Oechel, W. C.: Tundra carbon balance under varying temperature and moisture regimes, J. Geophys. Res., 115, G00I02, doi:10.1029/2009JG001237, 2010.

Hugelius, G., Strauss, J., Zubrzycki, S., Harden, J. W., Schuur, E. A. G., Ping, C.-L., Schirrmeister, L., Grosse, G., Michaelson, G. J., Koven, C. D., O'Donnell, J. A., Elberling, B., Mishra, U., Camill, P., Yu, Z., Palmtag, J., and Kuhry, P.: Estimated stocks of circumpolar permafrost carbon with quantified uncertainty ranges and identified data gaps, Biogeosciences, 11, 6573–6593, doi:10.5194/bg-11-6573-2014, 2014.

Huntington, T. G.: Evidence for intensification of the global water cycle: Review and synthesis, J. Hydrol., 319, 83–95, 2006.

Idso, S. B., Schmugge, T. J., Jackson, R. D., and Reginato, R. J.: The utility of surface temperature measurements for the remote sensing of surface soil water status, J. Geophys. Res., 80, 3044–3049, 1975.

Jia, G. J.: Greening of arctic Alaska, 1981–2001, Geophys. Res. Lett., 30, 2067, doi:10.1029/2003GL018268, 2003.

Johnson, L. C., Shaver, G. R., Giblin, A. E., Nadelhoffer, K. J., Rastetter, E. R., Laundre, J. A., and Murray, G. L.: Effects of drainage and temperature on carbon balance of tussock tundra microcosms, Oecologia, 108, 737–748, 1996.

Johnston, C. E., Ewing, S. A., Harden, J. W., Varner, R. K., Wickland, K. P., Koch, J. C., Fuller, C. C., Manies, K., and Jorgenson, M. T.: Effect of permafrost thaw on CO_2 and CH_4 exchange in a western Alaska peatland chronosequence, Environ. Res. Lett., 9, 085004, doi:10.1088/1748-9326/9/8/085004, 2014.

Jorgenson, M. T., Shur, Y. L., and Pullman, E. R.: Abrupt increase in permafrost degradation in Arctic Alaska, Geophys. Res. Lett., 33, L02503, doi:10.1029/2005GL024960, 2006.

Kattsov, V. M. and Walsh, J. E.: Twentieth-century trends of Arctic precipitation from observational data and a climate model simulation, J. Clim., 13, 1362–1370, 2000.

Kelley, J. J., Weaver, D. F., and Smith, B. P.: The variation of carbon dioxide under the snow in the Arctic, Ecology, 49, 358–361, 1968.

Kim, Y.: Effect of thaw depth on fluxes of CO_2 and CH_4 in manipulated Arctic coastal tundra of Barrow, Alaska, Sci. Total Environ., 505, 385–389, 2015.

Kirtman, B., Power, S. B., Adedoyin, J. A., Boer, G. J., Bojariu, R., Camilloni, I., Doblas-Reyes, F. J., Fiore, A. M., Kimoto, M., Meehl, G. A., Prather, M., Sarr, A., Schär, C., Sutton, R., Oldenborgh, G. J. van, Vecchi, G., and Wan, H. J.: Near-term Climate Change: Projections and Predictability, in Climate Change 2013: The Physical Science Basis, Contribution of Working Group I to the Fifth Assessment Report of the Intergovernmental Panel on Climate Change, Cambridge University Press, Cambridge and New York, 2013.

Koven, C. D., Ringeval, B., Friedlingstein, P., Ciais, P., Cadule, P., Khvorostyanov, D., Krinner, G., and Tarnocai, C.: Permafrost carbon-climate feedbacks accelerate global warming, P. Natl. Acad. Sci. USA, 108, 14769–14774, 2011.

Lakshmi, V., Jackson, T. J., and Zehrfuhs, D.: Soil moisture-temperature relationships: results from two field experiments, Hydrol. Process., 17, 3041–3057, 2003.

Lawrence, W. T. and Oechel, W. C.: Effects of soil temperature on the carbon exchange of taiga seedlings, II. Photosynthesis, respiration, and conductance, Can. J. For. Res., 13, 850–859, 1983.

Lee, H., Schuur, E. A. G., Inglett, K. S., Lavoie, M., and Chanton, J. P.: The rate of permafrost carbon release under aerobic and anaerobic conditions and its potential effects on climate, Glob. Change Biol., 18, 515–527, 2012.

Liljedahl, A. K., Boike, J., Daanen, R. P., Fedorov, A. N., Frost, G. V., Grosse, G., Hinzman, L. D., Iijma, Y., Jorgenson, J. C., Matveyeva, N., Necsoiu, M., Raynolds, M. K., Romanovsky, V. E., Schulla, J., Tape, K. D., Walker, D. A., Wilson, C. J., Yabuki, H., and Zona, D.: Pan-Arctic ice-wedge degradation in warming permafrost and its influence on tundra hydrology, Nat. Geosci., 9, 312–318, 2016.

Luus, K. A. and Lin, J. C.: The Polar Vegetation Photosynthesis and Respiration Model: a parsimonious, satellite-data-driven model of high-latitude CO_2 exchange, Geosci. Model Dev., 8, 2655–2674, doi:10.5194/gmd-8-2655-2015, 2015.

Mahadevan, P., Wofsy, S. C., Matross, D. M., Xiao, X., Dunn, A. L., Lin, J. C., Gerbig, C., Munger, J. W., Chow, V. Y., and Gottlieb, E. W.: A satellite-based biosphere parameterization for net ecosystem CO_2 exchange: Vegetation Photosynthesis and Respiration Model (VPRM), Global Biogeochem. Cy., 22, GB2005, doi:10.1029/2006GB002735, 2008.

Mastepanov, M., Sigsgaard, C., Dlugokenchy, E. J., Houweling, S., Ström, L., Tamstorf, M. P., and Christensen, T. R.: Large tundra methane burst during onset of freezing, Nature, 456, 628–630, 2008.

Mastepanov, M., Sigsgaard, C., Tagesson, T., Ström, L., Tamstorf, M. P., Lund, M., and Christensen, T. R.: Revisiting factors controlling methane emissions from high-Arctic tundra, Biogeosciences, 10, 5139–5158, doi:10.5194/bg-10-5139-2013, 2013.

McEwing, K. R., Fisher, J. P., and Zona, D.: Environmental and vegetation controls on the spatial variability of CH_4 emission from wet-sedge and tussock tundra ecosystems in the Arctic, Plant Soil, 388, 37–52, 2015.

Merbold, L., Kutsch, W. L., Corradi, C., Kolle, O., Rebmann, C., Stoy, P. C., Zimov, S. A., and Schulze, E. D.: Artificial drainage and associated carbon fluxes (CO_2 / CH_4) in a tundra ecosystem, Glob. Change Biol., 15, 2599–2614, 2009.

Myneni, R. B., Keeling, C. D., Tucker, C. J., Asrar, G., and Nemani, R. R.: Increased plant growth in the northern high latitudes from 1981 to 1991, Nature, 386, 698–702, 1997.

Natali, S. M., Schuur, E. A. G., Mauritz, M., Schade, J., Celis, G., Crummer, G., Johnston, C., Krapek, J., Pegoraro, E., Salmon, V., and Webb, E.: Permafrost thaw and soil moisture drive CO_2 and CH_4 release from upland tundra, J. Geophys. Res.-Biogeo., 120, 525–537, 2015.

Niinemets, Ü.: Responses of forest trees to single and multiple environmental stresses from seedlings to mature plants: Past stress

history, stress interactions, tolerance and acclimation, For. Ecol. Manage., 260, 1623–1639, 2010.

O'Donnell, J. A., Jorgenson, M. T., Harden, J. W., McGuire, A. D., Kanevskiy, M. Z., and Wickland, K. P.: The effects of permafrost thaw on soil hydrologic, thermal, and carbon dynamics in an Alaskan peatland, Ecosystems, 15, 213–229, 2011.

Oechel, W. C., Vourlitis, G. L., Hastings, S. J., Ault, R. P., and Bryant, P.: The effects of water table manipulation and elevated temperature on the net CO_2 flux of wet sedge tundra ecosystems, Glob. Change Biol., 4, 77–90, 1998.

Oechel, W. C., Vourlitis, G. L., Hastings, S. J., Zulueta, R. C., Hinzman, L., and Kane, D.: Acclimation of ecosystem CO_2 exchange in the Alaskan Arctic in response to decadal climate warming, Nature, 406, 978–981, 2000.

Olivas, P. C., Oberbauer, S. F., Tweedie, C. E., Oechel, W. C., and Kuchy, A.: Responses of CO_2 flux components of Alaskan Coastal Plain tundra to shifts in water table, J. Geophys. Res., 115, G00I05, doi:10.1029/2009jg001254, 2010.

Overland, J. E., Wang, M., Walsh, J. E., and Stroeve, J. C.: Future Arctic climate changes: Adaptation and mitigation time scales, Earth's Futur., 2, 68–74, 2014.

Panikov, N. S. and Dedysh, S. N.: Cold season CH_4 and CO_2 emission from boreal peat bogs (West Siberia): Winter fluxes and thaw activation dynamics, Global Biogeochem. Cy., 14, 1071–1080, 2000.

Parkin, T. B. and Venterea, R. T.: Chamber-based trace gas flux measurements, in: Sampling protocols, edited by: Follett, R. F., 3.1–3.39., 2010.

Peterson, K. M., Billings, W. D., and Reynolds, D. N.: Influence of water-table and atmospheric CO_2 concentration on the carbon balance of Arctic tundra, Arct. Alp. Res., 16, 331–335, 1984.

R Core Team: R: A language and environment for statistical computing, available from: http://www.r-project.org (last access: 20 June 2016), 2013.

Reginato, R. J., Idso, S. B., Vedder, J. F., Jackson, R. D., Blanchard, M. B., and Goettelman, R.: Soil water content and evaporation determined by thermal parameters obtained from ground-based and remote measurements, J. Geophys. Res., 81, 1617–1620, 1976.

Richards, J. A. and Xiuping, J.: Supervised classification techniques, in Remote sensing digital image analysis: an introduction, Springer-Verlag Berlin Heidelberg, 181–222, 1999.

Rochette, P. and Hutchinson, G. L.: Measurement of soil respiration in situ: chamber techniques, in Micrometeorology in Agricultural Systems, American Society of Agronomy, Madison, USA, 247–286, 2005.

Saugier, B., Roy, J., and Mooney, H. A.: Estimations of global terrestrial productivity: converging toward a single number?, in: Terrestrial Global Productivity, Elsevier, 543–557, 2001.

Schädel, C., Schuur, E. A. G., Bracho, R., Elberling, B., Knoblauch, C., Lee, H., Luo, Y., Shaver, G. R., and Turetsky, M. R.: Circumpolar assessment of permafrost C quality and its vulnerability over time using long-term incubation data, Glob. Change Biol., 20, 641–652, 2014.

Schaefer, K., Zhang, T., Bruhwiler, L., and Barrett, A. P.: Amount and timing of permafrost carbon release in response to climate warming, Tellus B, 63, 165–180, 2011.

Schuur, E. A. G., Bockheim, J., Canadell, J. G., Euskirchen, E., Field, C. B., Goryachkin, S. V., Hagemann, S., Kuhry, P., Lafleur, P. M., Lee, H., Mazhitova, G., Nelson, F. E., Rinke, A., Romanovsky, V. E., Shiklomanov, N., Tarnocai, C., Venevsky, S., Vogel, J. G., and Zimov, S. A.: Vulnerability of permafrost carbon to climate change: Implications for the global carbon cycle, Bioscience, 58, 701–714, 2008.

Schuur, E. A. G., Vogel, J. G., Crummer, K. G., Lee, H., Sickman, J. O., and Osterkamp, T. E.: The effect of permafrost thaw on old carbon release and net carbon exchange from tundra, Nature, 459, 556–559, 2009.

Schuur, E. A. G., McGuire, A. D., Schädel, C., Grosse, G., Harden, J. W., Hayes, D. J., Hugelius, G., Koven, C. D., Kuhry, P., Lawrence, D. M., Natali, S. M., Olefeldt, D., Romanovsky, V. E., Schaefer, K., Turetsky, M. R., Treat, C. C., and Vonk, J. E.: Climate change and the permafrost carbon feedback, Nature, 520, 171–179, 2015.

Schwarz, P. A., Fahey, T. J., and Dawson, T. E.: Seasonal air and soil temperature effects on photosynthesis in red spruce (Picea rubens) saplings, Tree Physiol., 17, 187–194, 1997.

Serreze, M. C., Walsh, J. E., III, F. S. C., Osterkamp, T., Dyurgerov, M., Romanovsky, V., Oechel, W. C., Morison, J., Zhang, T., and Barry, R. G.: Observational evidence of recent change in the northern high-latitude environment, Climate Change, 46, 159–207, 2000.

Shaver, G. R. and Jonasson, S.: Productivity of Arctic ecosystems, in: Terrestrial Global Productivity, Elsevier, 189–210, 2001.

Stafford, J. M., Wendler, G., and Curtis, J.: Temperature and precipitation of Alaska: 50 year trend analysis, Theor. Appl. Climatol., 67, 33–44, 2000.

Tarnocai, C., Canadell, J. G., Schuur, E. A. G., Kuhry, P., Mazhitova, G., Zimov, S., Tamocai, C., Canadell, J. G., Schuur, E. A. G., Kuhry, P., Mazhitova, G., Zimov, S., Tarnocai, C., Canadell, J. G., Schuur, E. A. G., Kuhry, P., Mazhitova, G., and Zimov, S.: Soil organic carbon pools in the northern circumpolar permafrost region, Global Biogeochem. Cy., 23, GB2023, doi:10.1029/2008GB003327, 2009.

Tscharntke, T., Hochberg, M. E., Rand, T. A., Resh, V. H., and Krauss, J.: Author sequence and credit for contributions in multiauthored publications, PLoS Biol., 5, e18, doi:10.1371/journal.pbio.0050018, 2007.

Webb, E. E., Schuur, E. A. G., Natali, S. M., Oken, K. L., Bracho, R., Krapek, J. P., Risk, D., and Nickerson, N. R.: Increased wintertime CO_2 loss as a result of sustained tundra warming, J. Geophys. Res., 121, 249–265, 2016.

White, M. A., Running, S. W., and Thornton, P. E.: The impact of growing-season length variability on carbon assimilation and evapotranspiration over 88 years in the eastern US deciduous forest, Int. J. Biometeorol., 42, 139–145, 1999.

Xia, J., Niu, S., Ciais, P., Janssens, I. A., Chen, J., Ammann, C., Arain, A., Blanken, P. D., Cescatti, A., Bonal, D., Buchmann, N., Curtis, P. S., Chen, S., Dong, J., Flanagan, L. B., Frankenberg, C., Georgiadis, T., Gough, C. M., Hui, D., Kiely, G., Li, J., Lund, M., Magliulo, V., Marcolla, B., Merbold, L., Montagnani, L., Moors, E. J., Olesen, J. E., Piao, S., Raschi, A., Roupsard, O., Suyker, A. E., Urbaniak, M., Vaccari, F. P., Varlagin, A., Vesala, T., Wilkinson, M., Weng, E., Wohlfahrt, G., Yan, L., and Luo, Y.: Joint control of terrestrial gross primary productivity by plant phenology and physiology, P. Natl. Acad. Sci. USA, 112, 2788–2793, 2015.

Xu, L., Myneni, R. B., Chapin III, F. S., Callaghan, T. V., Pinzon, J. E., Tucker, C. J., Zhu, Z., Bi, J., Ciais, P., Tømmervik, H., Euskirchen, E. S., Forbes, B. C., Piao, S. L., Anderson, B. T., Ganguly, S., Nemani, R. R., Goetz, S. J., Beck, P. S. A., Bunn, A. G., Cao, C., and Stroeve, J. C.: Temperature and vegetation seasonality diminishment over northern lands, Nature Climatic Change, 3, 581–586, 2013.

Zhou, T., Shi, P., Hui, D., and Luo, Y.: Global pattern of temperature sensitivity of soil heterotrophic respiration (Q_{10}) and its implications for carbon-climate feedback, J. Geophys. Res., 114, G02016, doi:10.1029/2008JG000850, 2009.

Zimov, S. A., Semiletov, I. P., Daviodov, S. P., Voropaev, Y. V., Prosyannikov, S. F., Wong, C. S., and Chan, Y.-H.: Wintertime CO_2 emission from soils of northeastern Siberia, Arctic, 46, 197–204, 1993.

Zimov, S. A., Davidov, S. P., Voropaev, Y. V., Prosiannikov, S. F., Semiletov, I. P., Chapin, M. C., and Chapin, F. S.: Siberian CO_2 efflux in winter as a CO_2 source and cause of seasonality in atmospheric CO_2, Climate Change, 33, 111–120, 1996.

Zona, D., Lipson, D. A., Zulueta, R. C., Oberbauer, S. F., and Oechel, W. C.: Microtopographic controls on ecosystem functioning in the Arctic Coastal Plain, J. Geophys. Res., 116, G00I08, doi:10.1029/2009JG001241, 2011.